EUROPEAN ORGANIZATION FOR NUCLEAR RESEARCH

CERN-EP/82-194
3 December 1982

EXPERIMENTAL STUDY OF THE NUCLEON STRUCTURE FUNCTIONS AND OF THE GLUON DISTRIBUTION FROM CHARGED-CURRENT NEUTRINO AND ANTINEUTRINO INTERACTIONS

CHARM Collaboration

F.Bergsma, J.Dorenbosch, M.Jonker, C.Nieuwenhuis and F.Udo
NIKHEF, Amsterdam, The Netherlands

J.V.Allaby, U.Amaldi, G.Barbiellini[1], L.Barone[2], A.Capone[2], W.Flegel, M.Metcalf, J.Panman and K.Winter
CERN, Geneva, Switzerland

I.Abt, J.Aspiazu, F.W.Büsser, H. Daumann, P.D.Gall, E.Metz, F.Niebergall, K.H.Ranitzsch and P.Stähelin
II. Institut für Experimentalphysik[3], Universität Hamburg, Hamburg, Germany

P.Gorbunov, E.Grigoriev, V.Kaftanov, V.Khovansky and A.Rosanov
Institute for Theoretical and Experimental Physics, Moscow, USSR

A.Baroncelli[4], B.Borgia[5], C.Bosio[4], M.Diemoz[5], U.Dore[5], F.Ferroni[5], E.Longo[5], P.Monacelli[5], F.de Notaristefani[5], P.Pistilli[5], C.Santoni[4], L.Tortora[4] and V.Valente[6]
Istituto Nazionale di Fisica Nucleare, Rome, Italy

(submitted to Physics Letters)

---

[1] On leave of absence from INFN, LN Frascati, Italy.

[2] On leave of absence from Istituto di Fisica, Università di Roma and INFN Sezione di Roma, Italy.

[3] Supported by Bundesministerium für Forschung und Technologie, Bonn, German Federal Republic.

[4] INFN Sezione Sanità and Istituto Superiore di Sanità, Rome, Italy.

[5] Istituto di Fisica, Università di Roma and INFN Sezione di Roma, Italy.

[6] Laboratori Nazionali INFN Frascati, Italy.

ABSTRACT

Inclusive neutrino and antineutrino charged current interactions were studied in the CHARM detector exposed to neutrino and antineutrino Wide Band Beams of the CERN 400 GeV SPS. The x and Q^2 dependence of the structure functions F_2 and xF_3 and of the antiquark momentum distribution q were determined.

The data have been interpreted in terms of QCD theory using the Furmanski-Petronzio method. In this way we have determined Λ_{LO}= [190 $^{+70}/_{-40}$ (stat) ± 70 (syst)] MeV and the structure functions of quarks and gluons without specific assumptions on their analytic dependence.

The results agree with previous experiments which relied on model assumptions in the analysis. We conclude that the model independent simultaneous analysis of the xF_3, F_2, q structure functions gives a more reliable determination of the gluon distribution in the nucleon.

We report on a study of the nucleon structure functions F_2 and xF_3 and the antiquark distribution measured as a function of x and Q^2, based on neutrino and antineutrino scattering on an isoscalar target. We analyzed the observed scaling violations, which manifest themselves as a characteristic Q^2-dependence of the quark and antiquark structure functions, in the framework of quantum chromodynamics. This theory predicts that the interaction of gluons with quarks which binds the hadrons also leads to scaling violations in the structure functions by gluon bremsstrahlung and by quark-antiquark pair production by gluons. The experimentally observed Q^2 dependence of the structure functions is directly related to the gluon momentum distribution. We used these measurements to determine the magnitude and the shape of the gluon distribution in the nucleon.

The data presented here were obtained using the CHARM fine-grain calorimeter exposed to the CERN 400 GeV SPS wide-band neutrino and antineutrino beams, providing high event-rate and covering a large neutrino energy domain. These features, combined with the capability of the detector to measure shower energies as low as 2 GeV, make it possible to explore a more extended kinematic region than in previous experiments.

Details of the apparatus and of its performance may be found in Ref.(1). The fine-grain target calorimeter consists of 78 equal subunits of marble plates ($CaCO_3$), scintillators and proportional drift tubes, surrounded by an iron frame magnet which serves as a calorimeter and muon spectrometer (*). The calorimeter is followed by a forward muon spectrometer consisting of iron disks with a toroidal magnetic field. Both the frame and the end magnets are

---

(*) In the antineutrino runs only two out of the four sides of the iron frames are magnetized in order to produce a dipolar field for simultaneous measurements of muon polarization.

instrumented with proportional drift tubes. We summarize the experimental resolution of the detector for the quantities used in the present study:

1. Hadronic energy: $\sigma(E_h)/E_h \sim 0.53/(E_h/\text{GeV})^{1/2}$

2. Muon momentum: $\sigma(p_\mu)/p_\mu \sim 15$ to 20%

3. Muon angle(*): $\sigma(\theta_\mu) \sim 5$ mrad for 50 GeV muons
   2 mrad for 150 GeV muons

The electronic trigger of the experiment required that at least four scintillator planes were hit and a total ionization energy larger than that produced by a 2.0 GeV shower was recorded. A long, penetrating track was required as a candidate for a muon.

This trigger is fully efficient for charged current neutrino interactions satisfying the following selection criteria in the analysis:

1. The interaction vertex lies within a fiducial volume covering a square of 240 × 240 cm^2 around the beam axis, and extending from plane 4 to 60, corresponding to a target mass of 82 tons.

2. The event contains no charged tracks entering the front or the side of the detector.

3. The event has a track identified as a muon associated with the interaction vertex. A track is defined as a muon if it shows no evidence of interaction and has a range corresponding to more than 1.0 GeV/c from the vertex.

(*) The resolution of the angle of muon tracks is averaged over event topologies and it includes the multiple scattering of the part of the track inside the shower.

4. The total energy of the event measured in the detector is larger than 10 GeV and smaller than 200 GeV.

In addition we required a fit of the muon trajectory observed in the spectrometers, selecting only the right-sign muons with a momentum larger than 2 GeV/c. To minimize the antineutrino (neutrino)-beam background in the neutrino (antineutrino) sample, events with a large computed error in the muon fit were also rejected. The final sample of events which passed all the selection criteria consists of ~ 50,000 neutrino and ~ 110,000 antineutrino events.

We obtained the momentum distribution functions of quarks and antiquarks in the nucleon by combining the two-dimensional event distribution in x and Q^2 for neutrinos and antineutrinos. In the analysis we assumed the validity of the Callan-Gross relation i.e. $F_2 = 2xF_1$. Fermi motion[2] and radiative correction[3] effects have been taken into account in the following analysis.

To obtain the momentum distributions one needs to know:

1. the relative shape of the neutrino and the antineutrino energy flux distributions;

2. the acceptance of the detector as a function of the relevant variables;

3. the effects of the experimental resolutions.

For point (1), we calculated the expected energy distribution of the beam using a Monte Carlo simulation of the beam optics combined with measurements of the parent spectra[4]. This predicted spectrum was then compared with the observed distribution of the total neutrino energy. We assumed, based on our previous measurements[5], that

$$\sigma_{CC}^{\nu} = 0.604 \cdot E_{\nu} \cdot 10^{-38} \text{cm}^2/\text{GeV} \qquad \sigma_{CC}^{\bar{\nu}} = 0.301 \cdot E_{\nu} \cdot 10^{-38} \text{cm}^2/\text{GeV}$$

over the energy range covered by this experiment (10-200 GeV), and

$$r = \sigma_{CC}^{\bar{\nu}} / \sigma_{CC}^{\nu} = 0.498 \pm 0.019$$

and used the predicted spectrum as input to a calculation which simulated the response of the apparatus. The comparison of the resulting spectrum with the observed neutrino energy distribution was then used to produce a refined prediction of the input spectrum. The simulation, together with our assumption on the ratio of the cross sections, also gives the relative normalisation of the neutrino and antineutrino event samples. We estimate a systematic uncertainty in this determination of the order of 4%. The Monte Carlo simulation used to evaluate the effects of the acceptance (point 2) and the finite resolution (point 3) was based on the measured resolutions and on the experimentally determined fitting efficiency for several topologies of the muon track.

The main problem of the analysis is connected with point (3) as a two dimensional unfolding of the experimental resolution is required. This problem is usually solved (see for example ref.[6]) by assuming a model for the structure functions as input for the Monte Carlo simulation. Comparing the input with the smeared output distribution, a correction factor for each two-dimensional bin can be determined.

The CHARM collaboration has developed a different method which makes use of a two-dimensional B-spline technique to determine resolution-unfolded functions representing $d^2\sigma/(dx \cdot dQ^2)$. This procedure has the advantage to be to a large extent model independent, but makes the interpretation of the results more difficult and their comparison with theoretical predictions less direct because the contents of the (x,Q^2) bins are correlated. Furthermore, although both methods work on the experimental distributions in E_h and x, the spline technique allows an analytical transformation from $F(x,E_h)$ to $F(x,Q^2)$, while for the first method only the mean value of Q^2 for each bin can be computed.

The resolution-unfolded functions representing $d^2\sigma/(dx \cdot dQ^2)$ have been obtained with the B-spline method following the recipe given in Ref. (7) for analysing the narrow band beam CHARM data. The results for $F_2(x,Q^2)$ and $xF_3(x,Q^2)$ are shown in Figs. 1a and 1b. The error bars also include the propagation of errors of the unfolding procedure. The trend of the two structure functions shows the well known shrinking with increasing Q^2, already observed in previous experiments[8].

In addition, the high statistics of this experiment makes it possible to determine the antiquark distribution function $q(x,Q^2)$, which we extracted from the antineutrino data at large y, using the relation

$$q(x) = d^2\sigma^{\bar{\nu}}/(dx\cdot dy) - (1-y)^2\cdot d^2\sigma^{\nu}/(dx\cdot dy)$$

for data with $y \geq 0.6$. The results are shown in Fig. 1c.

The interpretation of structure functions in terms of QCD predictions requires the integration of the Altarelli-Parisi equations[9]. These equations allow the determination of the structure functions at any value of the evolution variable $t \propto \ln \alpha_s(Q^2)/\alpha_s(Q_0^2)$ once one knows the distributions of quarks and gluons at some Q_0^2 $(t=0)$. Introducing $G(x,0)$,$V(x,0)$,$S(x,0)$ as the gluon, the valence quark and the sea quark x-distributions at $t = 0$, respectively, the experimental distributions can be expressed as:

$$xF_3(x,Q^2) = E_V(x,t)\circledcirc V(x,0) \tag{1.1}$$

$$F_2(x,Q^2) = E_{FF}(x,t)\circledcirc[V(x,0)+S(x,0)]+E_{FG}(x,t)\circledcirc G(x,0) \tag{1.2}$$

$$2\bar{q}(x,Q^2)=[E_{FF}(x,t)-E_V(x,t)]\circledcirc V(x,0)+E_{FF}(x,t)\circledcirc S(x,0)+E_{FG}(x,t)\circledcirc G(x,0) \tag{1.3}$$

where the $\circledcirc$ symbol denotes a convolution integral and $E_V(x,t)$, $E_{FF}(x,t)$, $E_{FG}(x,t)$ represent the evolution of non singlet (valence) quarks in themselves, of singlet quarks in singlet quarks and of singlet quarks in gluons respectively; they are determined by the Altarelli-Parisi equations once the scale parameter Λ is fixed. $V(x,0)$, $S(x,0)$ and $G(x,0)$ are not computable in the framework of perturbative QCD and have to be extracted from the experimental data together with Λ. Several numerical methods have been developed and used so far. They all require an explicit input parametrization of the x dependence of $V(x,0)$, $S(x,0)$, $G(x,0)$ at the reference value Q_0^2.

A different approach has been recently proposed by Furmanski and Petronzio[10], in which the analytical solution of the evolution equations is given in the form of a series of Laguerre polynomials in the variable $y=\ln(1/x)$, without

any prior knowledge of the particular analytic form of the x dependence of the functions V,S and G.

From Eq. (1.1) one notices that $V(x,0)$ can be determined from $xF_3(x,Q^2)$ alone. In this way a value of Λ can be extracted independently of S and G. The fit was performed to leading order using the data with $x \geq 0.03$ and $Q^2 \geq 3$ GeV^2, assuming contributions from four quark flavours and introducing the condition $xF_3(x) = 0$ for $x = 1$. The results of the fit are shown in Fig. 1a as continuous lines. The value of Λ_{LO} obtained from the best fit, including all corrections is $\Lambda_{LO} = (187\ ^{+130}/_{-110})$ MeV.

Because of the small number of parameters involved, the systematic uncertainties in the value of Λ_{LO} can best be studied for xF_3. We estimated the uncertainty by performing fits with different assumptions. The results are shown in table 1. We note that the more restrictive cut $Q^2 \geq 10$ GeV^2 does not change substantially the results of the fit, giving a value of $\Lambda_{LO} = (185\ ^{+150}/_{-120})$ MeV. From the first part of Table 1 we can estimate a global systematic uncertainty of 70 MeV. The final value of Λ_{LO} estimated from the non-singlet structure function is:

$$\Lambda_{LO} = [187\ ^{+130}/_{-110}\ (\text{stat.}) \pm 70\ (\text{syst.})]\ \text{MeV}$$

From the fitted distribution of xF_3 we evaluated the Gross-Llewellyn Smith sum-rule[11] and found , at $Q^2 = 10$ GeV^2:

$$\int_{0.0075}^{1} F_3(x)\cdot dx = 2.56 \pm 0.41 \ .$$

QCD predicts a value of $3\cdot(1 - \alpha_s/\pi) \simeq 2.8$, in good agreement with the experimental value.

We determined the gluon structure function by analysing simultaneously the three data sets appearing on the left hand side of Eq. (1). Different values of Λ_{LO} lead to different expressions for $V(x,0)$. We then introduced $V(x,0)$ and the

corresponding Λ_{LO} value in Eq. (1.2) and (1.3) and fitted simultaneously G(x,0) and S(x,0)(*). We assumed $S(x,t) = 0$ for $x \geq 0.5$. Consequently, G(x) and V(x) do not rely directly on data with $x \geq 0.5$, where the effects of Fermi motion and of experimental resolutions are large. In this way each value of Λ_{LO} corresponds to a set of distributions for V, G and S, and a total χ^2 value can be evaluated by comparing the right hand side of Eq. (1) with the data. From this χ^2 curve we can estimate

$$\Lambda_{LO} = [190\ ^{+70}/_{-40}\ (\text{stat.})\ \pm 70\ (\text{syst.})]\ \text{MeV}\ ,$$

in good agreement with the results obtained from the non singlet structure function alone. QCD is predicting small deviations from the Callan-Gross relation. Allowing for $R = (2xF_1-F_2)/2xF_1) = 0.1$ in the analysis, we found no significant change of the best value of Λ_{LO}.

The resulting fit is shown in Fig. 1b and 1c as continuous lines. In Fig 2 the x-dependence of the structure functions of the valence quarks, the sea quarks and the gluons are shown at different values of Q^2, as determined by the fit. Changes of the gluon structure function induced by reducing the antineutrino over neutrino flux ratio by its estimated uncertainty (4%) and by assuming $R = 0.1$ are shown in Fig. 3. We note that these variations hardly exceed the statistical uncertainties.

In summary, we have determined the structure functions F_2 and xF_3 and the q distribution using the B-spline technique. Using the Furmanski-Petronzio approach we have determined the Λ_{LO} parameter and the gluon momentum distribution in the nucleon. This picture of the nucleon structure is obtained for the first time without specific assumptions on the shape of the structure functions, both in the unfolding of the experimental resolutions and in the comparison with the Altarelli-Parisi QCD equations. The results agree with previous

---

(*) We assumed an SU(3) symmetric sea. The uncertainty introduced by this assumption is estimated to be small by other analysis[7,12].

experiments[8,12] which relied on model assumptions in the analysis. We conclude that this model independent simultaneous analysis of xF_3, F_2 and q structure functions gives a more reliable determination of the gluon distribution in the nucleon.

We gratefully acknowledge the competent help in data handling of W.M.v.Leeuwen and N.C.G.Macnacki (NIKHEF), of the staff of SARA (Amsterdam) and of J.Audier, C.Busi and G.De Bilio (CERN).

We wish to thank W.Furmanski and R.Petronzio for making their program for QCD analysis available to us and for useful discussions.

We also wish to express our gratitude to Dr. A.M.Wetherell for his contribution to this experiment.

REFERENCES

1. A.N.Diddens et al, CHARM Collaboration: Nucl. Instr. & Meth. 178 (1980) 27, and M.Jonker et al, CHARM Collaboration: Nucl. Instr. & Meth. 200 (1982) 183.

2. H.von Geramb, University of Hambourg, private communication J.P.Jeukenne, A.Lejenne and C.Mehaux: Phys. Rep. C25 (1976) 83.

3. A.de Rujula, R.Petronzio and A.Savoy-Navarro: Nucl. Phys. B154 (1979) 394.

4. C.Visser, NUBEAM, CERN HYDRA Application Library (1979)

5. M.Jonker et al, CHARM Collaboration: Phys. Lett. 99B (1981) 265.

6. J.G.H.de Groot et al, CDHS Collaboration: Z. Phys. C1 (1979) 143.

7. M.Jonker et al, CHARM Collaboration: Phys. Lett. 109B (1982) 133. J.Panman: PhD Thesis, University of Amsterdam (1981).

8. A review of previous results can be found, e.g. in J.Drees, "Proceedings 1981 International Symposium on Lepton and Photon Interactions at High Energies", Bonn (1981) p.474.

9. G.Altarelli and G.Parisi: Nucl. Phys. B126 (1977) 298.

10. W.Furmanski and R.Petronzio: Nucl.Phys. B195 (1982) 237

11. D.J.Gross and C.H.Llewellyn Smith: Nucl. Phys. B14 (1969) 337.

12. H.Abramowicz et al., CDHS Collaboration : Z. Phys. C12 (1982) 289.

TABLE 1

Sensitivity of Λ_{LO} from xF_3 fit to changes in the analysis.

Systematic uncertainties	$\Delta\Lambda_{LO}$
$\nu/\bar{\nu}$ flux ratio ± 4%	± 62 MeV
ν beam shape ± 5%(*)	± 33 MeV
$\bar{\nu}$ beam shape ± 5%(*)	± 5 MeV

Change in the analysis	$\Delta\Lambda_{LO}$
$Q^2 \geq 10$ GeV^2 (instead of 3 GeV^2)	- 2 MeV
$W^2 \geq 5$ GeV^2	- 30 MeV
No radiative corrections	- 24 MeV

(*) The beam shape has been varied by a multiplicative factor $w = 1 \pm \alpha \cdot E$ (GeV) corresponding to a maximum variation of 5% at E = 200 GeV.

FIGURE CAPTION

Fig. 1. Observed Q^2-dependence for xF_3 (a), F_2 (b) and q (c) for different x intervals. The error bars also include the propagation of errors of the unfolding procedure. The continuous curves are the results of the model independent QCD fit described in the text.

Fig. 2. 68% confidence contour of the x-dependence of valence quark (V), sea quark (S) and gluon (G) structure functions determined by the fit at $Q^2 = 3,10,20,50\ GeV^2$.

Fig. 3. Changes of the gluon structure function at $Q^2 = 10\ GeV^2$ by reducing the antineutrino over neutrino flux ratio by its estimated uncertainty of 4% (dashed line) and by assuming $R=(2xF_1-F_2)/2xF_1=0.1$ (dotted line). The full lines represent the best fit of the gluon distribution and one standard deviation of the statistical uncertainties.

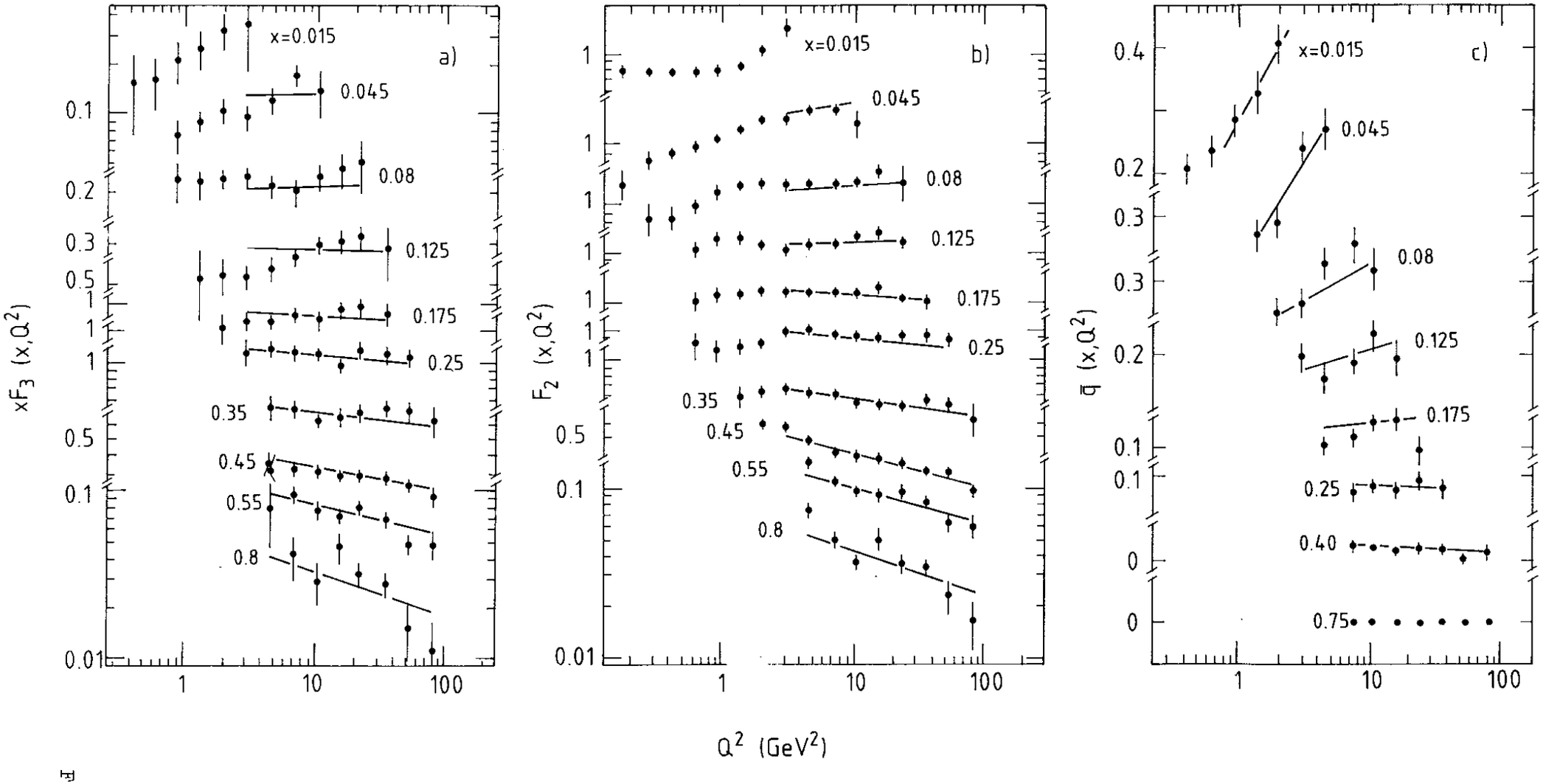
a)
b)
c)
x=0.015
0.045
0.08
0.125
0.175
0.25
0.35
0.45
0.55
0.8
0.40
0.75
$xF_3\ (x,Q^2)$
$F_2\ (x,Q^2)$
$\bar{q}\ (x,Q^2)$
$Q^2\ (GeV^2)$

Fig. 1

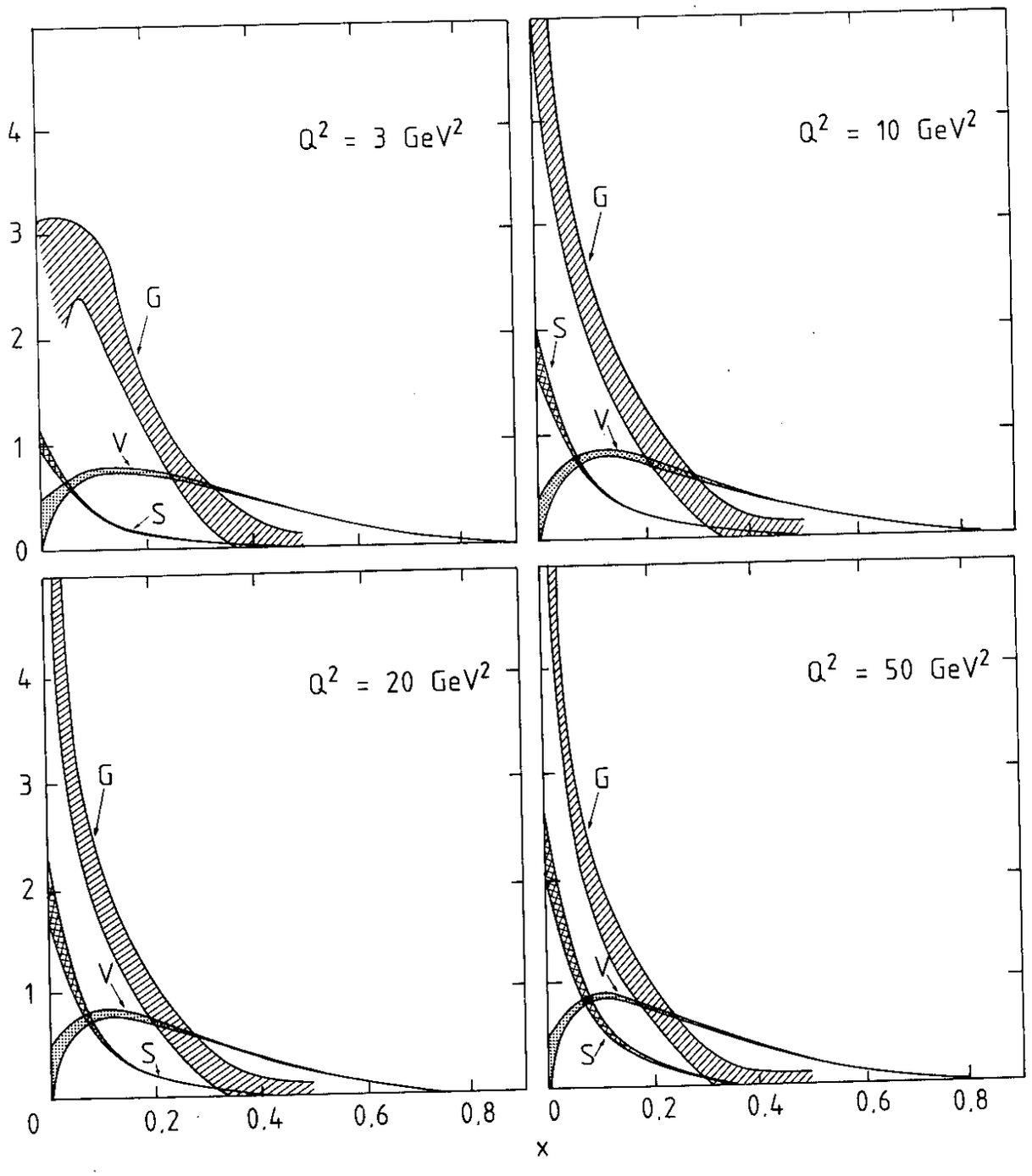

Fig. 2

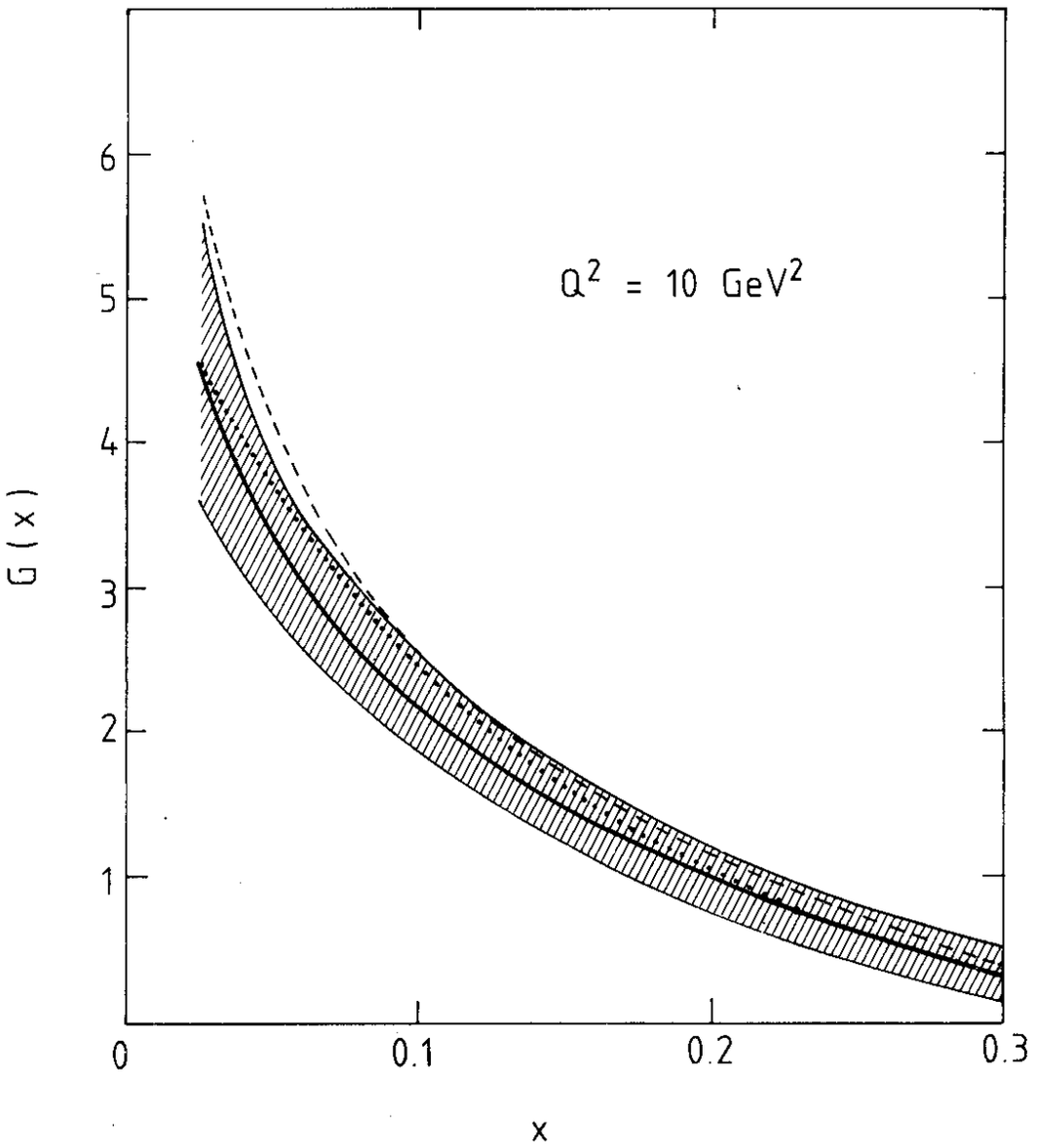

Fig. 3